TECHNICAL MEMORANDUMS

NATIONAL ADVISORY COMMITTEE FOR AERONAUTICS

No. 997

DETERMINATION OF THE BENDING AND BUCKLING EFFECT IN THE STRESS ANALYSIS OF SHELL STRUCTURES ACCESSIBLE FROM ONE SIDE ONLY

By A. Dose

Luftfahrtforschung
Vol. 18, Nos. 2-3, March 29, 1941
Verlag von R. Oldenbourg, München und Berlin

Washington
December 1941

NATIONAL ADVISORY COMMITTEE FOR AERONAUTICS

TECHNICAL MEMORANDUM NO. 997

DETERMINATION OF THE BENDING AND BUCKLING EFFECT IN THE STRESS ANALYSIS OF SHELL STRUCTURES ACCESSIBLE FROM ONE SIDE ONLY*

By A. Dose

SUMMARY

The present report describes a device for ascertaining the bending and buckling effect in stress measurements on shell structures accessible from one side only. Beginning with a discussion of the relationship between flexural strain and certain parameters, the respective errors of the test method for great or variable skin curvature within the test range are analyzed and illustrated by specimen example.

A. INTRODUCTION

The practical use of the data of individual strain measurements on thin-wall shell structures with the usual instrumental means, say, for checking the mathematical principles, is frequently open to question because of the disturbing effect of flexual strains induced by more or less severe bulging of the skin. Modern structural methods of air frames do not permit the elimination of flexural strains in many cases through measurements from two sides. These strains may be of considerable extent even though invisible to the naked eye. As a result the conventional strain gages do not always give reliable values for the strains in the median layer.

---

*"Untersuchungen zur Erfassung des Biegungs- bzw. Beulungseinflusses bei Spannungsmessungen an nur einseitig zugänglichen Schalenkonstruktionen." Luftfahrtforschung, vol. 18, nos. 2-3, March 29, 1941, pp. 95-101.

B. THEORY

a) Difference of Strain Between Median Plane and Neutral Fiber

The size of the flexural strain is most easily apparent from figure 1. A panel of thickness d is bent to a radius R in the middle layer without being strained, denoting the flexural strain occurring on the surface.

Assuming a linear law of distribution for the flexural strains, figure 1 yields the relation

$$\frac{l}{R} = \frac{l + \Delta l}{R + \frac{d}{2}}$$

hence

$$\frac{\Delta l}{l} = \epsilon = \frac{d}{2}\frac{1}{R} \qquad (1)$$

The ensuing arguments are based upon the assumption that the interior of the shell structure is inaccessible; hence the degree of bulging of the skin can only be ascertained from the outside.

Next visualize a device mounted on the bulged area of a shell with two fixed tips s millimeters apart and a movable center pin, the position of which shifts relative to the two other tips depending on the amount of curvature of the area. (See fig. 2.) If within this length the bulge is of circular shape, s becomes a chord of this circular shape. Then the height f of the bulge above a chord is an indication for the deflection of the surface in the particular test direction, for which, according to figure 3:

$$(r - f)^2 + \left(\frac{s}{2}\right)^2 = r^2$$

whence

$$r = \frac{f^2 + \left(\frac{s}{2}\right)^2}{2f} = R + \frac{d}{2} \tag{2}$$

or, for sufficiently small f:

$$R \approx \frac{\left(\frac{s}{2}\right)^2}{2f} - \frac{d}{2} \tag{3}$$

Thus the radius of curvature of the neutral layer can be defined according to equation (3) from the height f of the bulge, which can be measured by means of the device shown in figure 2.

Combining equations (1) and (2) gives

$$\epsilon = \frac{d\,f}{f^2 + \left(\frac{s}{2}\right)^2 - d\,f} \tag{4}$$

and, when neglecting the term with f^2:

$$\epsilon = \frac{d\,f}{\left(\frac{s}{2}\right)^2} \frac{1}{1 - \frac{d\,f}{\left(\frac{s}{2}\right)^2}} \tag{5}$$

For $\frac{d\,f}{\left(\frac{s}{2}\right)^2} < 1$, equation (5) gives, after expansion in series

$$\epsilon = \frac{d\,f}{\left(\frac{s}{2}\right)^2}\left[1 + \frac{d\,f}{\left(\frac{s}{2}\right)^2} + \ldots\right]$$

hence

$$\boxed{\epsilon \approx \frac{d\,f}{\left(\frac{s}{2}\right)^2}} \tag{6}$$

If the curvature is convex (fig. 3), f is positive.

The error of formula (6) is very small under ordinary conditions, as seen from the appended table.

TABLE I

ERROR OF EQUATION (6)

(d = 1 mm, $\frac{s}{2}$ = 10 mm)

f (mm)	$\epsilon \times 10^4$ equations (1) and (2)	$\epsilon \times 10^4$ equation (6)	$\Delta \epsilon \times 10^4$
0.1	10.01	10	0.01
.01	1.0001	1	.0001
.001	.100001	.1	.000001

If, under any loads, the deflection of the area rises from a value f_1 to a value f_2, the increment in flexural strain amounts to (fig. 4)

$$\epsilon = \frac{d}{\left(\frac{s}{2}\right)^2} (f_2 - f_1) \tag{7}$$

$$= \frac{d}{\left(\frac{s}{2}\right)^2} \Delta f \tag{8}$$

Now the curvometer illustrated in figure 2 can be combined with a strain gage. To this end, visualize the two fixed tips to be mounted movable so that - after rigid connection with the experimental object - they

yield to the strains of the body. Conforming to the length change of the two tips, equation (7) then should, strictly speaking, be written in the form

$$\epsilon = d\left[\frac{f_2}{\left(\frac{s_2}{2}\right)^2} - \frac{f_1}{\left(\frac{s_1}{2}\right)^2}\right]$$

But it becomes readily apparent that the difference of the two lengths s_1 and s_2 is usually negligibly small, so that equation (8) remains applicable.

The extent of the omissions in the derivation of equation (8) is illustrated on an example.

Supposing the curvature radius R_1 of a panel strip of 1 millimeter thickness changes to R_2 under continued strainless deflection of the median layer (fig. 5), so that the increment in surface bending strain can be readily computed from formula (1). It gives for

$$R_1 = 999.5 \text{ mm} \quad \text{and} \quad R_2 = 199.5 \text{ mm}$$

$$\epsilon_1 = 0.000500 \qquad \epsilon_2 = 0.002506$$

hence, according to equation (1)

$$\epsilon = \epsilon_2 - \epsilon_1 = +0.002006 = +20.06 \times 10^{-4} \qquad (9)$$

Next, assume that in state I of the body, a gage length of

I) 20 mm II) 10 mm (rise of arc)

is available. Arc length b_m of the median layer remains unchanged during transition from state I to state II according to assumption.

Then the quantities f_1, f_2; s_1, s_2 assume the following values:

a)		b)	
f_1 =	0.05000 mm	f_1 =	0.01250 mm
f_2 =	0.25096 mm	f_2 =	0.06275 mm
$\Delta f = f_2 - f_1$ =	+0.20096 mm	$\Delta f = f_2 - f_1$ =	+0.05025 mm
s_1 =	20.00000 mm	s_1 =	10.00000 mm
s_2 =	20.03205 mm	s_2 =	10.01904 mm
$s_2 - s_1$ =	+0.03205 mm	$s_2 - s_1$ =	+0.01904 mm

whence, according to approximate formula (8)

$$\begin{aligned} &\text{I)} \quad \epsilon = +0.002010 = +20.10 \times 10^{-4} \\ &\text{II)} \quad \epsilon = +0.002010 = +20.10 \times 10^{-4} \end{aligned} \tag{10}$$

The discrepancies ($\leqq$ 0.2 percent) between the results (9) and (10) are insignificant.

b) Effect of Shortening of Chord

Under the present curvature conditions it is important to bear in mind that in reality a tensometer merely records the change in chord length. So in the foregoing case a fictitiously attached instrument would, even under a strain-free deformation of the median layer, indicate a deflection the cause of which is the change in gage length due to the deflection. An increasing curvature is always indicated by an apparent negative strain.

Formulas and curves for predicting the amount of chord shortening are given. Under a deflection f of gage length s an apparent strain (fig. 6):

$$\epsilon = \frac{s - x}{s} \quad \text{occurs;} \tag{11}$$

in this case the formula (fig. 2)

$$\sin\left[\frac{180}{\pi}\,\frac{s}{2}\,\frac{2f}{f^2 + \left(\frac{x}{2}\right)^2}\right] = \left(\frac{x}{2}\right)\frac{2f}{f^2 + \left(\frac{x}{2}\right)^2} \tag{12}$$

is readily solved by approximation, and gives x and hence ϵ as function of f.

Equation (2) itself gives

$$r = \frac{f^2 + \left(\frac{s}{2}\right)^2}{2f}$$

with r as a function of f. This equation by sufficiently low f coincides very closely with an equilateral hyperbola, whereas equations (11) and (12) combined approximately to a parabola of the form

$$\epsilon \approx \frac{2}{3} \frac{f^2}{\left(\frac{s}{2}\right)^2} \tag{13}$$

The transcendental equation (12) [+ equation (11)] in the following range can be replaced with an error $|d\epsilon| \times 10^4 < 0.05$ by the formula (13):

gage length 10 mm $\quad 0 < |f| < \sim 0.3$ mm

gage length 20 mm $\quad 0 < |f| < \sim 0.6$ mm

as exemplified by the curves of figure 7.

In the example above the pertinent test instruments would have afforded a related strain

$$\left.\begin{aligned} \text{I)} \quad \epsilon &= \frac{s_2 - s_1}{s_1} = +0.001602 = +16.02 \times 10^{-4} \\ \text{II)} \quad \epsilon &= \frac{s_2 - s_1}{s_1} = +0.001904 = +19.04 \times 10^{-4} \end{aligned}\right\} \tag{14}$$

as against $+20.06 \times 10^{-4}$ according to equation (9). This appreciable difference is removed if the correction factors $(-\Delta\epsilon)$

$$\left.\begin{aligned} \text{I)} \quad \epsilon_2 &= -4.23 \times 10^{-4} \\ \epsilon_1 &= -\ .16 \times 10^{-4} \\ \hline \Delta\epsilon &= -4.07 \times 10^{-4} \end{aligned}\right. \qquad \left.\begin{aligned} \text{II)} \quad \epsilon_2 &= -1.02 \times 10^{-4} \\ \epsilon_1 &= -\ .04 \times 10^{-4} \\ \hline \Delta\epsilon &= -0.98 \times 10^{-4} \end{aligned}\right\} \tag{15}$$

read from the curves of figure 7 are applied to the values of equation (14), resulting in practically complete agreement with equation (9) and (10), respectively.

Since the effect of shortened chord length can, according to this, become very serious, it is recommended for smaller curvature radii to secure these by means of a suitable instrument such as figure 2, and to allow for the apparent ϵ of figure 7, or else resort to shorter gage lengths. But it has no effect on the result, whether arc a) $b = 20.00034$, b) $b = 10.00004$ replaces s_1 in the denominator of equation (14).

However, in many strain measurements the solution of quantities Δf, that is, the use of equation (8) will be sufficient.

c) Penetration of Tips

Further it is necessary to find the correction factor to be applied to equation (8) as a result of the penetration of the tips in the skin. The aim in all strain measurements will be a minimum and constant initial pressure consistent with the solid seating of the instrument. The depth of penetration, of course, is of so much greater influence as the panel thickness is less. It may depend also upon the type and thickness of the plating layer if Al-Cu-Mg alloys are involved.

The determination of such factors is withheld for the present, pending a special study.

d) Variation of Curvature

The present arguments were always based on the assumption that the particular object within the gage length of the tensometer resembles in its form a simple arc of a circle. The following lines are dedicated to the extent to which the application of the equation, especially equation (8), is justified for bulge-height curves of varying curvatures within range of the tensometer gage length.

To this end several computations for the 10 and 20 millimeter gage length were carried out, of which figure 8 illustrates a sector of the bulge-height curves on a

cylindrical duralumin panel (wall thickness of skin = 0.6 mm) stiffened in pressure direction. These conditions are now simulated in somewhat modified form for the subsequent study:

An originally flat sheet panel of thickness d = 1 millimeter is so bent that its median layer - without undergoing any strain - follows the equation

$$y = A \sin\left(2\pi \frac{x}{\lambda}\right) \tag{16}$$

with A = 1.5 millimeters, λ = 100 millimeters (fig. 9).

It is readily apparent that in this instance extreme curvatures occur similar to those used in the earlier example.

The problem now is divided into

I. An exact calculation of the flexural strain at the surface by integration,

II. Calculation of resultant strain for the same zone according to equations (1) and (8), respectively

The latter is termed the "three-point method" for short. For purposes of comparison both computations are made: once, for the standard gage length l of the Huggenberger tensometer of 20 millimeters, then, for l = 10 millimeters.

In order to limit the scope of the calculations, these are made at only one point of the sine curve, that is, in the zone of maximum change of $1/\rho$, with ρ the radius of the curvature. According to figure 10, the desired place of the function $1/\rho$ is close to 65°.

I. Integral method.- The strain at the surface is readily defined. From figure 11

$$\frac{d\Delta b}{d v} = \frac{d}{2} \tag{17}$$

is readily deduced; whence the total lengthening of the

arc for an interval denoted by numerals 1 and 2 amounts to

$$\Delta b = \frac{d}{2}\int_{\nu_1}^{\nu_2} d\nu \tag{18}$$

and the angle of the normal ν follows the relation

$$\tan \nu = -\frac{1}{y'} = -\frac{1}{A\frac{2\pi}{\lambda}\cos\left(\frac{2\pi}{\lambda}x\right)} \qquad \text{(cf. equation (16))}$$

Then:

$$\frac{1}{\cos^2\nu}\,d\nu = -\frac{\frac{2\pi}{\lambda}\sin\left(\frac{2\pi}{\lambda}x\right)}{A\frac{2\pi}{\lambda}\cos^2\left(\frac{2\pi}{\lambda}x\right)}\,dx$$

and

$$d\nu = -\frac{A\frac{4\pi^2}{\lambda^2}\sin\left(\frac{2\pi}{\lambda}x\right)}{1 + A^2\frac{4\pi^2}{\lambda^2}\cos^2\left(\frac{2\pi}{\lambda}x\right)}\,dx \tag{19}$$

Equation (18) then gives

$$\Delta b = -\frac{d}{2}A\frac{4\pi^2}{\lambda^2}\int_{x_1}^{x_2}\frac{\sin\left(\frac{2\pi}{\lambda}x\right)}{1 + A^2\frac{4\pi^2}{\lambda^2}\cos^2\left(\frac{2\pi}{\lambda}x\right)}\,dx \tag{20}$$

With the aid of the transformation

$$\left.\begin{aligned} z &= A\frac{2\pi}{\lambda}\cos\left(\frac{2\pi}{\lambda}x\right) \\ dz &= -A\frac{4\pi^2}{\lambda^2}\sin\left(\frac{2\pi}{\lambda}x\right)dx \end{aligned}\right\} \tag{21}$$

we get

$$\Delta b = \frac{d}{2}\int_{z_1}^{z_2} \frac{1}{1 + z^2}\, dz = \left[\frac{d}{2} \text{ arc tan } z\right]_{z_1}^{z_2} \qquad (22)$$

while the reinsertion of equation (21) in equation (22) finally gives

$$\Delta b = \left\{\frac{d}{2} \text{ arc tan } \left[A\,\frac{2\pi}{\lambda} \cos\left(\frac{2\pi}{\lambda} x\right)\right]\right\}_{x_1}^{x_2} \qquad (23)$$

with the related strain at

$$\epsilon_{integr} = \frac{\Delta b}{b} \qquad (24)$$

where b follows from the sine curve at

$$b = \int_{x_1}^{x_2} \sqrt{1 + y'^2}\, dx = \int_{x_1}^{x_2} \sqrt{1 + A^2\,\frac{4\pi^2}{\lambda^2} \cos^2\left(\frac{2\pi}{\lambda} x\right)}\, dx \qquad (25)$$

Equation (25) can be reduced to the elliptic integral of the second category

$$E(\varphi, k) = \int_0^{\varphi} \sqrt{1 - k^2 \sin^2 \varphi}\, d\varphi$$

$$b = \int_{x_1}^{x_2} \sqrt{1 + \frac{A^2\,4\pi^2}{\lambda^2} - A^2\,\frac{4\pi^2}{\lambda^2} \sin^2\left(\frac{2\pi}{\lambda} x\right)}\, dx$$

$$= \sqrt{1 + \frac{A^2\,4\pi^2}{\lambda^2}} \int_{x_1}^{x_2} \sqrt{1 - \frac{A^2\,\frac{4\pi^2}{\lambda^2}}{1 + A^2\,\frac{4\pi^2}{\lambda^2}} \sin^2\left(\frac{2\pi}{\lambda} x\right)}\, dx$$

Putting

$$\varphi = \frac{2\pi}{\lambda} x. \quad d\varphi = \frac{2\pi}{\lambda} dx$$

then gives

$$b = \frac{\lambda}{2\pi} \sqrt{1 + \frac{A^2 4\pi^2}{\lambda^2}} \int_{\varphi_1}^{\varphi_2} \sqrt{1 - k^2 \sin^2 \varphi} \, d\varphi \qquad (26)$$

with the abbreviation

$$k^2 = \frac{A^2 \frac{4\pi^2}{\lambda^2}}{1 + \frac{A^2 4\pi^2}{\lambda^2}} \qquad (27)$$

In this manner the strain in a certain test zone is obtained by equations (23), (24), and (25).

II. Three-point method.- This method is most easily explained by means of figure 12. The desired bending strain is found from the curvature radius of the median layer by means of equation (1) instead of equation (8). The value is secured in the following manner: Assume that the points bounding the arc b (equation (25)) of the median layer have the coordinates (x_1, y_1) and (x_2, y_2). Then define the coordinates of point P_3 (x_3, y_3) in figure 12, located on the one hand, on the median perpendicular of the chord $P_1 P_2$ and on the sine curve, on the other. The equation of the perpendicular reads:

$$x = -\frac{m}{y_m} y + x_m + m \qquad (28)$$

where

$$\frac{m}{y_m} = \frac{y_2 - y_1}{x_2 - x_1} \qquad (29)$$

The intersection P_3 follows from the insertion of equation (28) in equation (16). The solution of this transcendental equation by approximation gives y_3, and equation (28) the related x_3. Next, the radius of a circle placed through the points P_1, P_2, and P_3 must be defined. With x_M, y_M as coordinates of the center of the circle, we get the three equations

$$(x_n - x_M)^2 + (y_n - y_M)^2 = R^2; \quad n = 1, 2, 3 \qquad (30)$$

from which x_M, y_M, and R can be computed.

Hence $\epsilon_{3\,points}$ itself is known.

The following relates the result of the numerical computations, where, as already emphasized, the bulge-height curve (according to equation (16)) at the point corresponding to the angle $\alpha = 65^\circ$ is to be subjected to closer study. Table II contains the numerical data for the median layer.

TABLE II

DATA FOR MEDIAN LAYER (EQUATION (16)) IN THE RANGE OF THE TEST POINT

x mm	$\left(\frac{2\pi}{\lambda} x\right)^\circ$	y mm	R cm	1/R cm^{-1}
6	21.6	0.5522	46.40	0.0216
7	25.2	.6387	40.11	.0249
8	28.8	.7227	36.00	.0278
9	32.4	.8037	31.84	.0314
10	36.0	.8817	28.99	.0345
11	39.6	.9561	26.74	.0374
12	43.2	1.0268	24.86	.0402
13	46.8	1.0935	23.29	.0429
14	50.4	1.1558	22.05	.0454
15	54.0	1.2135	21.02	.0476
16	57.6	1.2665	20.12	.0497
17	61.2	1.3145	19.37	.0516
18	64.8	1.3572	18.74	.0534
19	68.4	1.3947	18.21	.0549
20	72.0	1.4267	17.78	.0562
21	75.6	1.4529	17.47	.0572
22	79.2	1.4735	17.22	.0581
23	82.8	1.4882	17.04	.0587
24	86.4	1.4970	16.95	.0590
25	90.0	1.5000	16.89	.0592
26	93.6	1.4970	16.95	.0590
27	97.2	1.4882	17.04	.0587

According to this tabulation, the curvature radius of the sine curve within the explored piece ranges between 46.40 and 17.04 centimeters. The calculations refer, as previously indicated, once, to a gage length of around 20 millimeters, and then, to about 10 millimeters, the selected limiting points being:

a) 20 millimeter gage length b) 10 millimeter gage length

$x_1 = 6$, $y_1 = 0.5522$ mm $x_1 = 11$, $y_1 = 0.9561$ mm

$x_2 = 26$, $y_2 = 1.4970$ mm $x_2 = 21$, $y_2 = 1.4529$ mm

Equations (23) and (25) give for the cited interval:

a) $\Delta b = 0.04666$ mm b) $\Delta b = 0.02453$ mm

$b = 20.0301$ mm $b = 10.0134$ mm*

hence, according to equation (24):

a) $\epsilon_{integr} = 0.002330$ b) $\epsilon_{integr} = 0.002450$ (31)

According to the three-point method

a) $R = 207.55$ mm b) $R = 202.42$ mm

which, according to table II, closely approach the R relating to $x = 16$.

Whence, according to equation (1) with $\frac{d}{2} = 0.5$ mm

a) $\epsilon_{3points} = 0.002409$ b) $\epsilon_{3points} = 0.002470$ (32)

A comparison of the results (equations (31) and (32) reveals departures from the true value to the amount of

a) $\Delta\epsilon = 0.000079$ b) $\Delta\epsilon = 0.000020$

or $\Delta\epsilon_{20} = 3.4$ percent $\Delta\epsilon_{10} = .8$ percent

*The values for the elliptic integrals were obtained by interpolation from Legendre's Tables (published by F. Emde, Stuttgart, 1931).

In view of the not inconsiderable buckling of the sheet, the experimental findings can be summed up to the effect that the standard 20-millimeter gage length of the extensively employed Huggenberger tensometer (type A) will fail only in very extreme cases.

That the sine formula chosen for the buckling curve actually reproduces the curvature conditions of the initially considered true buckling curves (fig. 8) is readily apparent from a harmonic analysis of the pertinent piece of the curve.

The use of 12 ordinates afforded

$$\left.\begin{aligned} y_{mm} = {} & -0.216 + 0.358 \cos\left(\frac{2\pi}{\lambda} x\right) \\ & - 0.165 \cos\left(2\,\frac{2\pi}{\lambda} x\right) + 0.028 \cos\left(3\,\frac{2\pi}{\lambda} x\right) \\ & - 0.010 \cos\left(4\,\frac{2\pi}{\lambda} x\right) + 0.007 \cos\left(5\,\frac{2\pi}{\lambda} x\right) \\ & - 0.002 \cos\left(6\,\frac{2\pi}{\lambda} x\right) \\ & - 1.634 \sin\left(\frac{2\pi}{\lambda} x\right) - 0.120 \sin\left(2\,\frac{2\pi}{\lambda} x\right) \\ & - 0.024 \sin\left(3\,\frac{2\pi}{\lambda} x\right) + 0.004 \sin\left(4\,\frac{2\pi}{\lambda} x\right) \\ & - 0.002 \sin\left(5\,\frac{2\pi}{\lambda} x\right) \end{aligned}\right\} \quad (33)$$

the greatest term of which is

$$y = -1.634 \sin\left(\frac{2\pi}{\lambda} x\right) \quad (\lambda = 111.9 \text{ mm}). \quad (34)$$

C. CURVOMETER AS AUXILIARY DEVICE FOR TENSOMETERS - APPLICATION

Following the description of the method of securing the flexural strain by observation of the height of the bulge, its practical application merely requires an

auxiliary device, attached to a tensometer, which enables an accurate record of the deflection of the test area. A number of such instruments to fit the Huggenberger tensometer of 20-millimeter gage length were constructed in the experimental section of the Focke-Wulf Aircraft Company. The motion of a movable tip at midcenter is reproduced at about 125 amplifications by a pointer on a scale. Other instruments with greater amplification ($i \approx 450$) also are being constructed.

The essential characteristic of the proposed method is that the curvature measurements are made concurrently with the strain measurements. (German patent applied for.) The use of a device developed by Dr. A. Huggenberger as well as of others operating on similar principles is, for several reasons, not recommended on thin-wall shell structures. (See Rötscher-Jaschke, Auswertung von Dehnungsmessungen, Berlin 1939, pp. 88-91.)

Suppose strain measurements have been made on the surface of a shell by the known Wys' method with 4 test directions a, b, c, d, whereby $a \perp c$, $b \perp d$, and angle $(a,b) = 45°$. Then it is readily seen from Eulers' formula for the curvature of a surface, according to which

$$\frac{1}{R_a} + \frac{1}{R_c} = \frac{1}{R_b} + \frac{1}{R_d} \tag{35}$$

that the computed bending strain and recorded height of bulge, respectively, must approximately satisfy a corresponding summation formula, that is, according to equation (8)

$$\Delta f_a + \Delta f_c = \Delta f_b + \Delta f_d \tag{36}$$

It is to be noted that for great curvatures or curvature changes the ϵ values obtained by tensometer cannot - because of the effect illustrated in figure 7 - satisfy the invariance condition of the ϵ sum of two directions at right angles to each other at one point - instrumental errors discounted altogether - as proved by a test with a Huggenberger tensometer of 20-millimeter gage length with attached curvometer. The test specimen was a 120 x 350 x 0.5 millimeter steel sheet fastened at the top of an arc made of wood and bent to $R \approx 200$

millimeters by applying weights (P = 0 to 2 kg). The readings were made on the tensometer at 0 and 2 kilogram load. The area around the gage length was polished before testing. The test data are given in table III.

As is seen, the experimental ϵ values of the condition $\epsilon_a + \epsilon_c = \epsilon_b + \epsilon_d$ are satisfied only after applying the corrections from equation (15).

The extent to which the flexural strains can distort the desired stress distribution pattern is illustrated by a measurement on a wing-span web (Al-Cu-Mg alloy, s = 0.75 mm): the uncorrected ϵ values gave the principal stress values shown in figure 14 b, while the ϵ values corrected for bulging (according to equation (8)) are shown in figure 14 a. The corresponding numerical values are given in table IV.

TABLE IV

NUMERICAL VALUES TO FIGURE 14

a)	σ_1 =	-678	kg/cm^2	b) -1060	kg/cm^2
	σ_2 =	558	kg/cm^2	460	kg/cm^2
	$\lvert\tau_{max}\rvert$ =	618	kg/cm^2	760	kg/cm^2
	α =	-37.5°		-36.4°	

In the case of simple longitudinal stresses in struts, etc., the test method also assumes satisfactory results at places not accessible from both sides.

Translation by J. Vanier,
National Advisory Committee
for Aeronautics.

TABLE III

STRAIN MEASUREMENTS ON STEEL SHEET (AIRCRAFT MATERIAL 1263.1, d ≈ 0.5+ mm) OF VARYING CURVATURE

	Test direction a	c	b	d	a + c	b + d	Δ percent*	Remarks
Δf mm	0.205	0.003	0.111	0.097	0.208	0.208	0	curvometer
Δf mm	.200	.002	.108	.094	.202	.202	0	$\frac{1}{1000}$ mm dial gage
f_1 mm	.044	.003	.013	.033	.047	.046	1	$\frac{1}{1000}$ mm dial gage
f_2 mm	.249	.006	.124	.130	.255	.254	.2	$f_1 + \Delta f$ curvometer
$\Delta\epsilon \times 10^4$	4.	0	1.01	1.05	4.	2.06	___	(equation 13)
$\epsilon \times 10^4$	7.87	0.02	5.14	4.24	7.89	9.38	8.6	tensometer
$\epsilon_{correct} \times 10^4$	11.87	.02	6.15	5.29	11.89	11.44	1.9	$\epsilon + \Delta\epsilon$

* Δ percent $= \left| \frac{(a + c) - (b + d)}{\Sigma(a + c + b + d)} \right| \times 100$

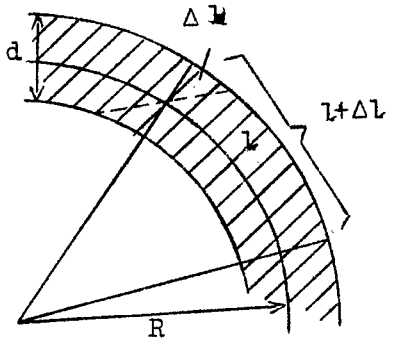

Figure 1.-Explanation of eq. (1).

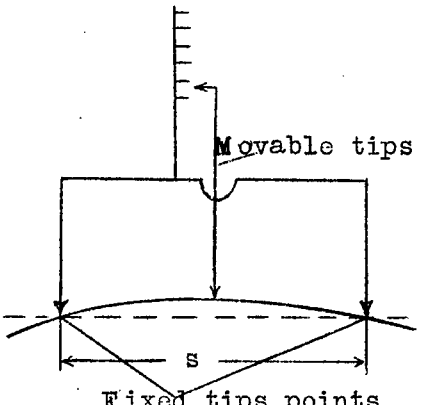

Figure 2.-Curvature meter.

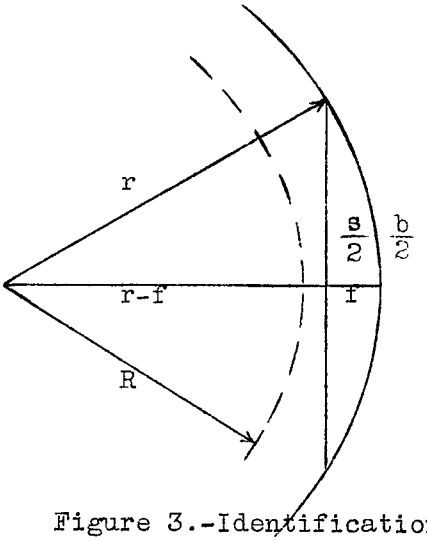

Figure 3.-Identification of height f of bulge.

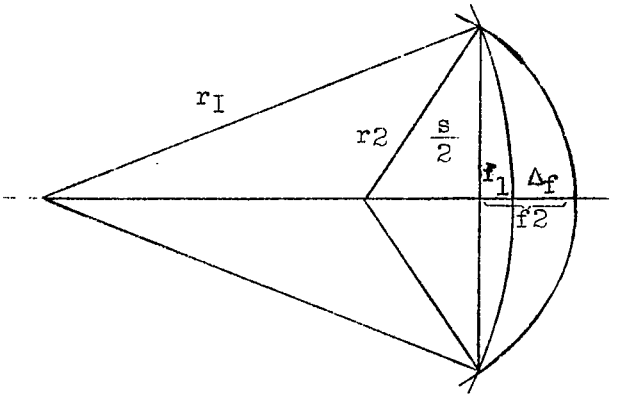

Figure 4.-Indentification of eq. (8).

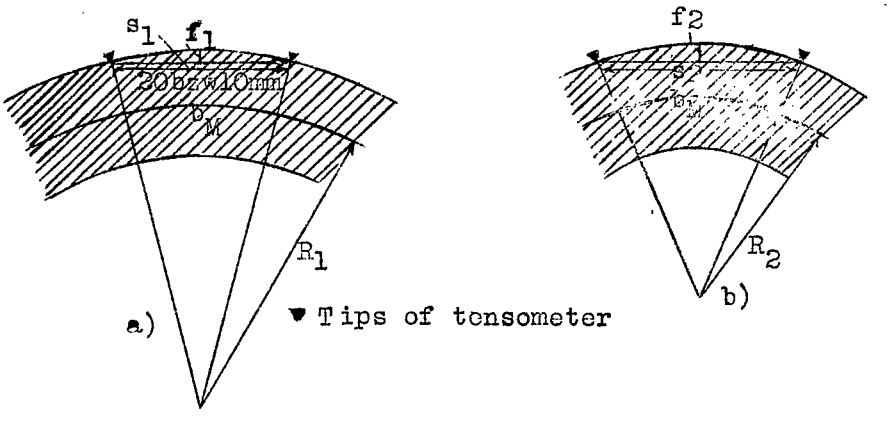

Figure 5.-Indentification of numerical example.
a) State 1, b) state 2.

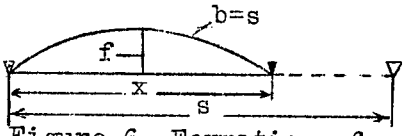

Figure 6.-Formation of an apparent ϵ in bending.

▽ On final setting of tips.
▼ Setting after start of bulging

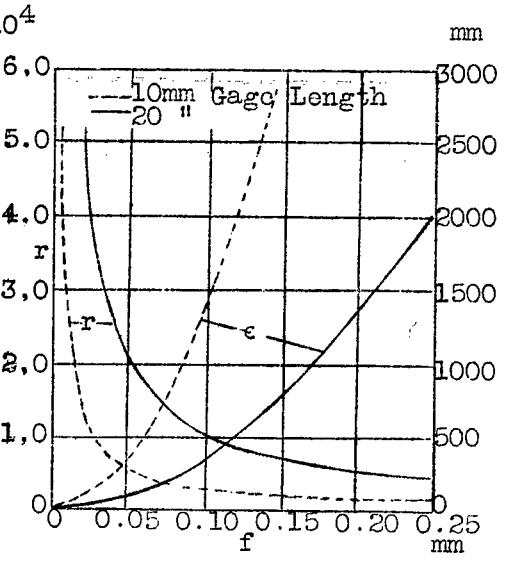

Figure 7.-Apparent ϵ indicated on tensometer under severe deflection of skin.

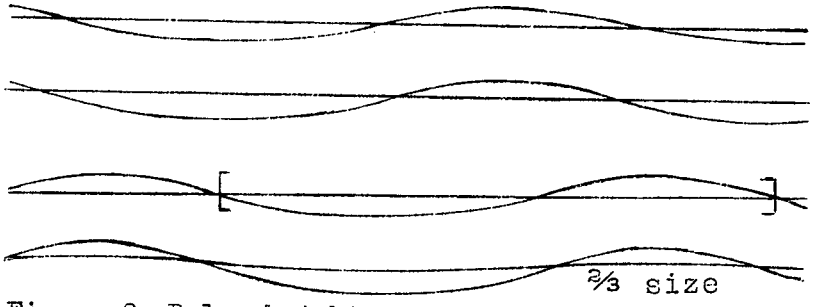

Figure 8.-Bulge-height curves of a compressed cylindrical panel of aircraft material 3116.5(bulging between stiffeners, original curves 2.7 :1).

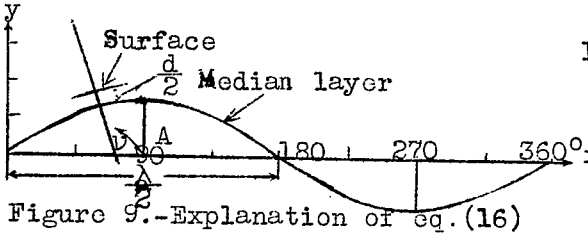

Figure 9.-Explanation of eq.(16)

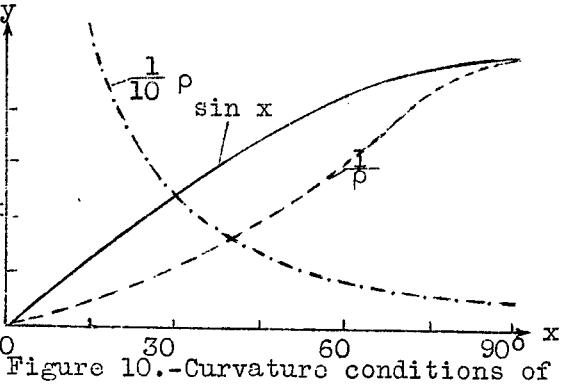

Figure 10.-Curvature conditions of curve y = sin x

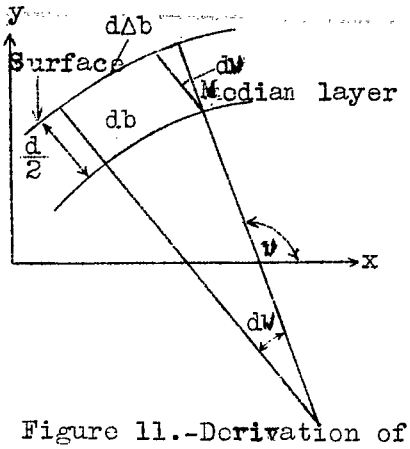

Figure 11.-Derivation of bending strain at surface of sinusoidally curved sheet.

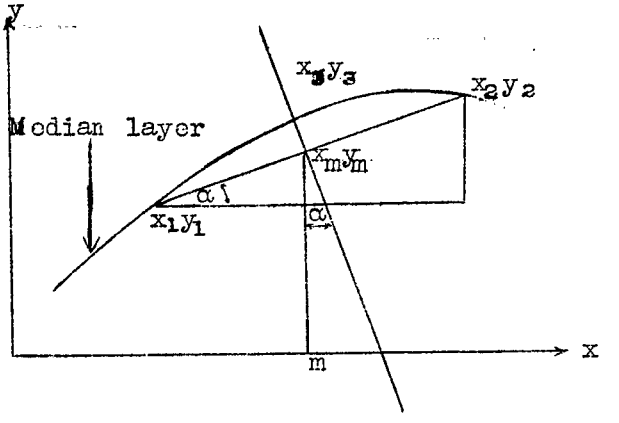

Figure 12.-Illustration of three-point method.

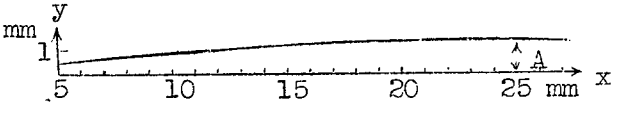

Figure 13.-Arc length of median layer (enlarged)(c.f. table 2).

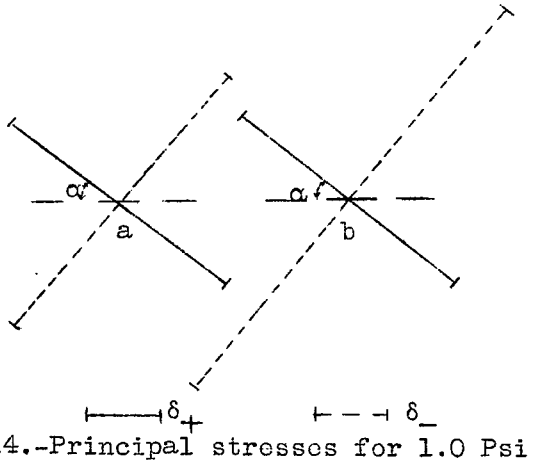

Figure 14.-Principal stresses for 1.0 Psi, $E=70\times10^4 kg/cm^2$, $\mu = 0,3$.

a) From ϵ-values corrected for buckling.
b) From uncorrected ϵ-values.